

Finite-Thickness and Charge Relaxation in Double-Layer Interactions

Aldemar Torres and René van Roij
Institute for Theoretical Physics, Utrecht University
Leuvenlaan 4, 3584 CE Utrecht, The Netherlands.

Gabriel Téllez
Departamento de Física, Universidad de Los Andes
A. A. 4976 Bogotá, Colombia.

Abstract

We extend the classical Gouy-Chapman model of two planar parallel interacting double-layers, which is used as a first approximation to describe the force between colloidal particles, by considering the finite-thickness of the colloids. The formation of two additional double layers due to this finite thickness, modifies the interaction force compared to the Gouy-Chapman case, in which the colloids are semi-infinite objects. In this paper we calculate this interaction force and some other size-dependent properties using a mean field level of description, based on the Poisson-Boltzmann (PB) equation. We show that in the case of finite-size colloids, this equation can be set in a closed form depending on the geometrical parameters and on their surface charge. The corresponding linear (Debye-Hückel) theory and the well-known results for semi-infinite colloids are recovered from this formal solution after taking appropriate limits. We use a density functional corresponding to the PB level of description to show how in the case when the total colloidal charge is fixed, it redistribute itself on their surfaces to minimize the energy of the system depending on the afore mentioned parameters. We study how this charge relaxation affects the colloidal interactions.

1 Introduction

Electrostatic forces play a remarkable role in the stabilization and phase behavior of colloidal suspensions. Thus, it is not surprising that understanding the interaction among charged colloidal particles across an intervening electrolyte solution has been an important goal for colloid science since the pioneering work by Verwey and Overbeek [1]. Poisson-Boltzmann theory (PB) allows a mean field calculation of these interaction at a nonlinear level. The corresponding linearized description, Debye-Hückel theory (DH), is exact in the asymptotic

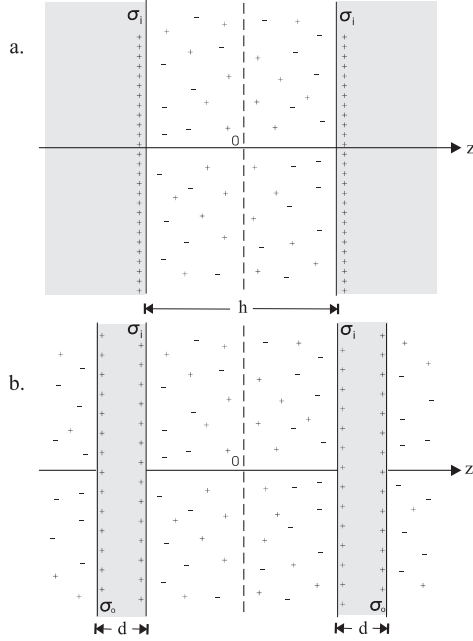


Figure 1: a) Two parallel double-layers. b) Four double-layers as a model for colloidal interactions. Here the finite size of the colloids is taken into account.

limit of infinite dilutions and low-charged colloids, when the electrostatic interactions are weak compared to the thermal energy. DH theory fails to describe quantitatively the thermodynamic properties of realistic colloidal suspensions, and nonlinear PB equation must be employed, often at the expense of numerical computations.

Nonetheless, the PB equation admits analytical solution in some non-trivial cases. An important example is that in which two parallel infinite double-layers interact. In this case the geometry is dictated by two planar objects (colloids) which are infinite in the directions parallel to their surface and semi-infinite in one direction perpendicular to their surface, and carrying a surface charge σ . The region between the semi-infinite objects is filled with symmetric electrolyte as illustrated in figure 1a. Thus, the force between the colloids is mediated by the diffuse layers surrounding their surface. PB theory allows the calculation of this force as well as the free energy of interaction, through the determination of the mean local electrostatic potential in the region filled with electrolyte [1]. The planar geometry is relevant for colloidal spheres in the case that the Debye length of the electrolyte is much smaller than the radius of the spheres (such that the curvature effects are unimportant). It is also relevant for understanding of colloidal clay platelets and their interactions. An important aspect of these clay platelets is their finite thickness d which can easily be of the same order as

the Debye length and which could therefore affect the plate-plate interactions.

The geometry of interest in this paper is depicted in figure 1b, showing the finite thickness of the platelets and hence two inner surfaces (with charge density σ_i) and two outer surfaces (with charge density σ_o). Since the plates are completely immersed in electrolyte, double-layers form at both sides of the colloidal particles. The presence of charge on the outer surfaces induces the redistribution of ions in the electrolyte, and diffuse layers of charge appear in the vicinity of each region in contact with the colloids. In other words, the finite-size of the colloidal particles allows the formation and interaction of four double-layers instead of two. It is clear that in this case, the force between the colloidal particles depends not only on their relative separation h but also on their thickness d .

In the traditional model of two interacting double layers [1], the initial studies supposed a fixed surface charge density or a fixed potential at the surfaces. But there have been several studies in which the surface charge of the colloidal planes is not fixed, but a charge regulation mechanism can occur [2, 3], due to an ion adsorption-desorption of the colloidal surface groups. When the finite-thickness of the colloids is taken into account, as in our model (see figure 1b), there is another kind of charge regulation that can take place. The total charge of each colloid can be fixed but the amounts of charge on the inner and outer surfaces can vary in order to minimize the thermodynamic grand potential of the system. We call this mechanism “charge relaxation”. This charge relaxation also affects the force between the colloids. In this contribution, we study quantitatively these finite-size effects in the case of two equally charged colloids immersed in a symmetrical electrolyte, in the framework of PB theory. The present nonlinear study already accounts for charge renormalization effects [4, 5, 6, 7].

In section 2 we specify the model and introduce a suitable density functional. In section 3, the nonlinear PB equation is solved. We show that for the geometry of figure 1b, the solution of the PB equation can be set in a convenient analytical closed form, which depends only on the geometrical parameters h and d and on the total surface charge density σ of the colloids. The linear DH potential is obtained from the formal analytical solution by taking the appropriate limits. In section 4, we minimize the density functional to calculate the fraction of charge on the inner and outer surfaces, as a function of the aforementioned parameters, when charge relaxation is allowed. Results are discussed in section 5 and conclusions are given in section 6.

2 The model

We consider four infinite parallel planes located at $z_1 = -h/2 - d$, $z_2 = -h/2$, $z_3 = h/2$ and $z_4 = h/2 + d$, with surface charge densities σ_1 , σ_2 , σ_3 , σ_4 respectively. The regions $z_1 < z < z_2$ correspond to the interior of the left colloid, and $z_3 < z < z_4$ to the interior of the right colloid. The regions outside the colloids are filled with an electrolyte solution of dielectric constant ϵ , at temperature T . Inside the colloids there is no electrolyte present but there is a medium with the

same dielectric constant as the electrolyte solution to avoid electrostatic image effects. The system is assumed to be in contact with a salt reservoir of salt density ρ_s such that the electrolyte has screening length $l_D = \kappa^{-1} = (8\pi\lambda_B\rho_s)^{-1/2}$, with $\lambda_B = e^2/(k_B T \varepsilon)$ the Bjerrum length, where e is the elementary charge, k_B Boltzmann constant, and ε the electric permittivity of the solvent. In what follows, all lengths will be conveniently given in units of the Debye length, namely $D = \kappa d$, $H = \kappa h$ and $x = \kappa z$. For simplicity we consider the case when $\sigma_1 = \sigma_4 = \sigma_o$ and $\sigma_2 = \sigma_3 = \sigma_i$ as illustrated in figure 1b. Note that with these conditions the system possess mirror symmetry with respect to the plane at $x = 0$ sketched with dashed lines.

The thermodynamic and statistical properties of the system are characterized by the dimensionless grand potential density functional $\omega[\rho] \equiv \kappa\beta\Omega[\rho]/(2A\rho_s)$ where A is the area of the planes and Ω is the grand potential density functional. $\omega[\rho]$ is given by

$$\omega[\rho] = \omega_{id}[\rho] + \frac{1}{2} \int dx \rho(x) \phi(x) + 2f(\chi \log \chi + (1 - \chi) \log(1 - \chi)). \quad (1)$$

The first term in the right hand side is the ideal gas entropic contribution of the ions in the solution,

$$\omega_{id}[\rho] = \frac{1}{2\rho_s} \sum_{\alpha=\pm} \int dx \rho_\alpha(x) \left(\log \left(\frac{\rho_\alpha(x)}{\rho_s} \right) - 1 \right), \quad (2)$$

where $\rho_+(x)$ and $\rho_-(x)$ are the number density profiles of the positive and negative salt ions respectively. The second term of (1) accounts for the electrostatic energy, with $\phi(x) = e\psi(x)/k_B T$ the reduced electrostatic potential (ψ is the electrostatic potential), and the total number charge in the system defined as

$$\rho(x) = \rho_+(x) - \rho_-(x) + \frac{\kappa}{e} \sum_{j=1}^4 \sigma_j \delta(x - x_j). \quad (3)$$

The last term in (1) is of entropic origin and takes into account the fact that the surface charge ions on the colloids are indistinguishable. For later convenience we have introduced $\chi = \sigma_i/\sigma$ which is the fraction of charge in the inner surface with respect to the total charge density on a colloid $\sigma = \sigma_i + \sigma_o$. Finally, the dimensionless constant $f = 4\pi\lambda_B\sigma/(e\kappa)$ is the ratio of the Debye length $l_D = 1/\kappa$ and the Gouy-Chapman length $\Lambda = e/(4\pi\sigma\lambda_B)$. The later is the decay length of the counterions distribution around an infinite charged plane with bare surface charge density σ in the salt free limit $\rho_s \rightarrow 0$. Note that f is an estimate of the electrostatic energy compared to the characteristic energy of thermal fluctuations in the system.

Minimization of the density functional (1) with respect to the ion density profiles $\rho_\pm(x)$ gives the equilibrium density profiles in terms of the average local potential. In the mean field approach the reduced local electric potential $\phi(x)$ is the solution of the nonlinear Poisson–Boltzmann equation

$$\frac{d^2\phi}{dx^2} = \sinh \phi \quad \text{in the outside} \quad (4)$$

$$\frac{d^2\phi}{dx^2} = 0 \quad \text{in the inside} \quad (5)$$

with the boundary conditions that ϕ is a continuous function of x and

$$\phi'(\frac{H}{2}^-) - \phi'(\frac{H}{2}^+) = f_i \quad (6a)$$

$$\phi'((\frac{H}{2} + D)^-) - \phi'((\frac{H}{2} + D)^+) = f_o \quad (6b)$$

$$\lim_{|x| \rightarrow \infty} \phi'(x) = 0 \quad (6c)$$

with $f_i = 4\pi l_B \sigma_i / (e\kappa)$, $f_o = 4\pi l_B \sigma_o / (e\kappa)$ as explained before.

The functional (1) evaluated for the equilibrium profiles gives the equilibrium dimensionless grand potential. Further minimization of the later quantity with respect to the parameter $\chi = \sigma_i / \sigma$ allows to find the fraction of charge on each surface, when charge relaxation is allowed. This will be discussed in section 4. The DH level of description can be obtained by expanding (1) to second order in the density and linearizing (4) for $|\phi| \ll 1$. It can also be obtained from the nonlinear solution as will be discussed next.

3 Solution of Poisson-Boltzmann equation

3.1 The Nonlinear PB Equation

Due to the mirror symmetry it is sufficient to consider $x \geq 0$ since the potential is an even function of x : $\phi(x) = \phi(-x)$. Also, without loss of generality, we consider positively charged colloids i.e. $f_i > 0$. The solution of the PB equation in the region $-H/2 < x < H/2$ with the boundary conditions $\phi(0) = \phi_0$ and $\phi'(0) = 0$ is well-known. There are several different but equivalent expressions for this solution [1, 3, 8, 9]. After the usual first integration of the PB equation and using the boundary condition at $x = 0$ we have

$$\phi'(x)^2 = 4 \left(\sinh^2 \frac{\phi(x)}{2} - \sinh^2 \frac{\phi_0}{2} \right). \quad (7)$$

From this equation we see that $\sinh^2 \frac{\phi(x)}{2} > \sinh^2 \frac{\phi_0}{2}$, thus $|\phi(x)| > |\phi_0|$. We deduce that $\phi(x)$ does not change its sign. Furthermore with the choice $f_i > 0$, we have $\phi(x) \geq \phi_0$, and then $\phi'(x) \geq 0$.

Integrating once again with respect to x and defining $t = \sinh(\phi/2)$, the integral can be set in the form

$$x = \int_{\sinh(\phi_0/2)}^{\sinh(\phi(x)/2)} \frac{dt}{\sqrt{(t^2 + 1)(t^2 - \sinh^2(\phi_0/2))}}. \quad (8)$$

One recognizes an elliptic integral of the first kind [10], defined as

$$F(\theta, k) = \int_0^\theta \frac{d\alpha}{\sqrt{1 - k^2 \sin^2 \alpha}}, \quad (9)$$

and hence we have

$$x = \frac{1}{\cosh(\phi_0/2)} F\left(\arccos \frac{\sinh(\phi_0/2)}{\sinh(\phi(x)/2)}, \frac{1}{\cosh(\phi_0/2)}\right). \quad (10)$$

An inversion yields

$$\sinh \frac{\phi(x)}{2} = \frac{\sinh(\phi_0/2)}{\text{cn}(x \cosh(\phi_0/2), k)}, \quad (11)$$

where cn is the Jacobian cosine amplitude. The modulus $k = 1/\cosh(\phi_0/2)$ of the elliptic functions will not be explicitly indicated in the following to lighten the notation. To take into account the finite-size of the colloids, we match this expression with the solutions in the regions $H/2 < x < H/2 + D$ and $H/2 + D < x$. We get

$$\phi(x) = \phi_1(x) = 2 \sinh^{-1} \left[\frac{\sinh(\phi_0/2)}{\text{cn}(x \cosh(\phi_0/2))} \right] \quad \text{for } 0 \leq x \leq H/2 \quad (12)$$

$$\phi(x) = \phi_2(x) = a \left(x - \frac{H}{2} \right) + \phi_1(H/2) \quad \text{for } H/2 \leq x \leq H/2 + D \quad (13)$$

with the dimensionless electric field inside the colloids given by

$$a = 2 \sinh(\phi_0/2) \text{sc} \left(\frac{H}{2} \cosh \frac{\phi_0}{2} \right) - f_i. \quad (14)$$

For the outside region $x > H/2 + D$ we find

$$\phi(x) = \phi_3(x) = 2 \ln \frac{1 + Ce^{-x}}{1 - Ce^{-x}} \quad \text{for } H/2 + D \leq x, \quad (15)$$

with

$$C = \tanh(\phi_2(\frac{H}{2} + D)/4) e^{\frac{H}{2} + D}, \quad (16)$$

where $\text{sc}(u, k) = \text{sn}(u, k)/\text{cn}(u, k)$ with $\text{sn}(u, k)$ the Jacobian sine amplitude [10, 12]. For a fixed ϕ_0 equations (12), (13) and (15) give the exact analytic form of the mean field within the Poisson-Boltzmann theory. To completely specify the spatial dependence of ϕ , we still need to determine its value at the origin ϕ_0 . For this we use the boundary conditions (6) to get

$$\frac{f_o + f_i}{2} = \sinh \left[\frac{aD}{2} + \sinh^{-1} \left(\frac{\sinh(\phi_0/2)}{\text{cn}(\frac{H}{2} \cosh \frac{\phi_0}{2})} \right) \right] + \sinh(\phi_0/2) \text{sc} \left(\frac{H}{2} \cosh \frac{\phi_0}{2} \right) \quad (17)$$

with a given by eq. (14).

For given values of the parameters f_i , f_o , H and D , equation (17) can be easily solved numerically for ϕ_0 [11]. In combination with (12) to (16) it gives the exact mean field as a function of f_i , f_o , and the geometrical parameters H and D .

An interesting feature of $\phi_1(x)$ as given in (12) is that if we consider the prolongation of the function ϕ_1 in eq. (12), for any value of x , from the general properties of the elliptic function cn , we notice that ϕ_1 is a periodic function of x with period $4K$, where $K = F(\pi/2, k)$. For $x > 0$, it has a first pole at the first positive zero of cn , at $x = K/(\cosh(\phi_0/2))$. Physically, the potential should be bounded. This means that for a given separation H , ϕ_0 satisfies

$$H < H_{\max} = \frac{2K}{\cosh(\phi_0/2)}. \quad (18)$$

The case $H = H_{\max}$ corresponds to a situation where the surface charge $\sigma_i \rightarrow +\infty$. Eq. (18) serves as a guide to choose the initial value for ϕ_0 in the numerical resolution of (17), or in a direct numerical integration of Poisson–Boltzmann equation (4).

3.2 The Linear Regime: Debye–Hückel Theory

We can recover the results from the linear Debye–Hückel theory by taking the limit $\phi_0 \ll 1$. In that limit the modulus of the elliptic functions $k \rightarrow 1$. Using $\text{cn}(u, 1) = 1/\cosh u$, we have $\phi_1(x) = \phi_0 \cosh x$ for $\phi_0 \ll 1$, which is the solution of the linear problem in the region $0 \leq x \leq H/2$. Similarly, using $\text{sn}(u, 1) = \tanh u$ we have

$$a = \phi_0 \sinh(H/2) - f_i, \quad (19)$$

and equation (17) reduces to a linear equation which can be easily solved for ϕ_0 . The result is

$$\phi_0 = \frac{f_o + (1 + D)f_i}{e^{H/2} + D \sinh(H/2)}. \quad (20)$$

The last equation in combination with (19) and the expression for $\phi_1(x)$, determines also the potential in the region $H/2 \leq x \leq H/2 + D$, namely, $\phi_2(x) = a(x - H/2) + \phi_1(H/2)$. Finally, linearizing (15) and (16) we get $\phi_3(x) = [aD + \phi_1(H/2)]e^{H/2+D}e^{-x}$. It is an easy exercise to show that the same expressions can be obtained with the DH approximation taken ab initio. For that, it is enough to take functions of the form $\phi_1(x) = Ae^x + Be^{-x}$, $\phi_2(x) = a(x - H/2) + \phi_1(H/2)$ and $\phi_3(x) = Ce^{H/2+D}e^{-x}$. Using the boundary conditions and the continuity of the potential, a system of coupled linear equations for the constants A, B, C and a is obtained. The solution coincides with the exact nonlinear solution in the limit of small potentials.

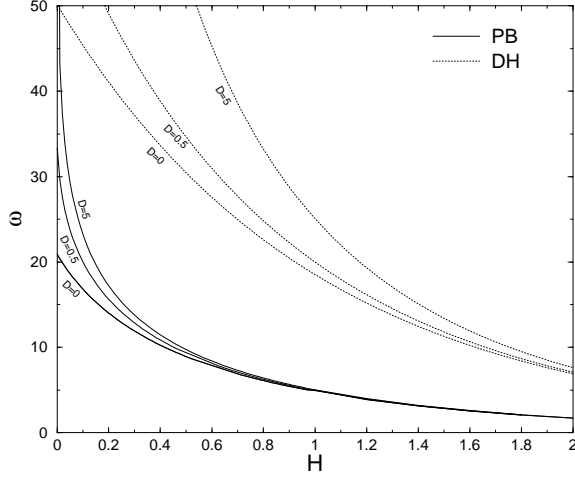


Figure 2: Exact and DH based equilibrium grand potential as a function of the separation distance H for two interacting finite-size planes. In this plot $\chi = 0.5$ and $f = 10$.

4 The Equilibrium Grand Potential

As mentioned before, the total charge on the colloids is assumed to be fixed, but eventually different fractions of charge can move between the inner and outer surfaces. We took this into account in the density functional (1) by fixing the total charge on the colloids instead of the surface charge on the inner and outer surfaces separately, through the introduction of the charge fraction χ . The functional (1) evaluated at the equilibrium density profile gives, for fixed χ , the grand potential of the system. Further minimization of the later quantity with respect to χ allow us to find the fraction of charge on each surface that minimizes the equilibrium grand potential. The grand potential is obtained by inserting the expressions (12), (13) and (15) into the density functional (1). The explicit calculation involves well-known quadratures of the Jacobian elliptic functions, in particular

$$\int \frac{du}{\text{cn}^2(u, k)} = \frac{\text{sc}(u, k) \text{dn}(u, k) - E(\text{am}(u, k), k)}{1 - k^2} + u, \quad (21)$$

where $\text{dn}(u, k)$ is the Jacobian delta amplitude, $E(x, k)$ the elliptic integral of second kind and $\text{am}(u, k)$ the Jacobian amplitude [10, 12]. After some calculations we obtain

$$\begin{aligned} \omega = & 2\phi(H/2) \sinh(\phi_0/2) \text{sc}(H/2k) - 8 \cosh(\phi_0/2) \text{sc}(H/2k) \text{dn}(H/2k) \\ & + 8E(\text{am}(H/2k), k) \cosh(\phi_0/2) - 2H \sinh^2(\phi_0/2) \\ & + 2 \sinh(\phi(\frac{H}{2} + D)/2) \phi(\frac{H}{2} + D) - 16 \sinh^2(\phi(\frac{H}{2} + D)/4) \\ & + f[2\chi \ln \chi + 2(1 - \chi) \ln(1 - \chi) + \chi \phi(H/2) + (1 - \chi) \phi(\frac{H}{2} + D)]. \end{aligned} \quad (22)$$

Notice that $k = 1/\cosh(\phi_0/2)$, that $\phi(x)$ can be evaluated from (12), (13), (15), and that ϕ_0 is the solution of (17) and thus depends on χ . For given values of H , D and f we determine the value of χ that minimizes the grand potential (22) numerically [11].

The DH level of description is obtained from the linear density functional corresponding to (1). In this case the dimensionless grand potential reads

$$\omega = f[2\chi \ln \chi + 2(1 - \chi) \ln(1 - \chi) + \chi\phi(H/2) + (1 - \chi)\phi(\frac{H}{2} + D)] \quad (23)$$

where ϕ is given by the expressions derived in section 3.2. Although equations (22) and (23) are a bit involved, the grand potential has the familiar repulsive form as that for semi-infinite colloids. This is illustrated in figure 2, where the linear and nonlinear results are compared for the case $f = 10$ and $\chi = 0.5$. Some consequences of the size-dependence of the potential will be discussed in the next section.

5 Results

5.1 Charge relaxation

Let us first consider the aforementioned effect of charge relaxation, in which charges can move between the colloidal surfaces. We shall refer to this as the annealed case, in contrast to the case in which equal amounts of charge are fixed (“quenched”) on the inner and outer surfaces. Notice that in the quenched case $\chi = \sigma_i/\sigma = 0.5$. In figure 3, the charge fraction χ is plotted as a function of the colloid separation H for different colloidal thicknesses. We observe that for inter-colloidal separations of the order of the Debye length, a fraction of charge moves to the outer surface. This effect substantially increases with increasing values of the parameter f , as we can conclude from the inset, which shows the fraction of charge at $H \rightarrow 0$. Notice that for increasing f , the values of χ at contact tend faster to zero. Thus, the effect of increasing f is similar to what we observe in the main plot when D is increased, namely, a more pronounced relaxation of charge toward the outer surface. Notice that this effect already disappears at colloidal separations of the order of two times the Debye length, at which a small difference with the quenched case is observed. It also worth to mention the fact that in the main plot, no substantial change is observed when the thickness is increased from $D = 5$ to $D = 10$. In fact, for a given value of $H \neq 0$, when the thickness varies from $D = 5$ to $D = \infty$, the charge fraction χ does not change beyond 3%. For a colloidal thickness of a few Debye lengths, the distance to the outer surface is already too large to affect the fraction of charge that migrates as we vary the distance between the colloids.

5.2 Electrostatic potential

In figure 4 we plot the electrostatic potential $\phi(x)$ for $x > 0$ in the quenched case, obtained by equations (12-15) using the methods described in section 3. The

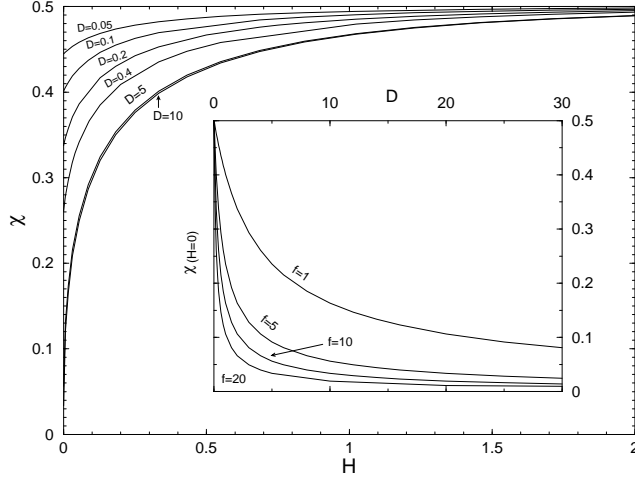


Figure 3: Fraction of surface charge density χ as a function of colloid separation for different colloidal sizes for $f = 10$. In the inset we see how $\chi(H \rightarrow 0)$ changes with varying f .

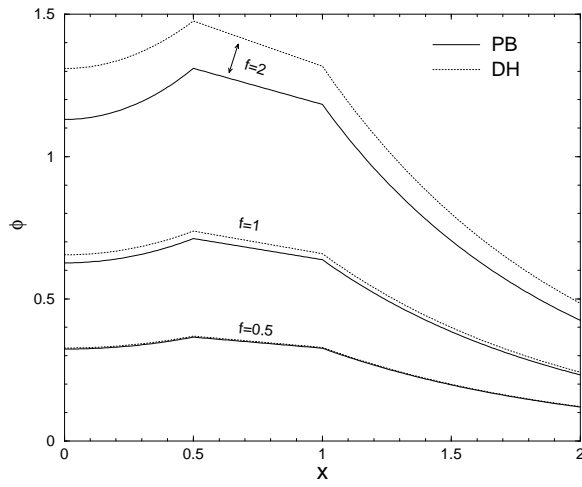


Figure 4: Average local electrostatic potential for $H = 1$, $D = 0.5$ and $\chi = 0.5$ (quenched case). Different values of the dimensionless parameter f are plotted. Notice that the linear DH results are asymptotically exact in the limit $f \ll 1$ but fail to quantitatively predict the local mean field for $f \geq 1$.

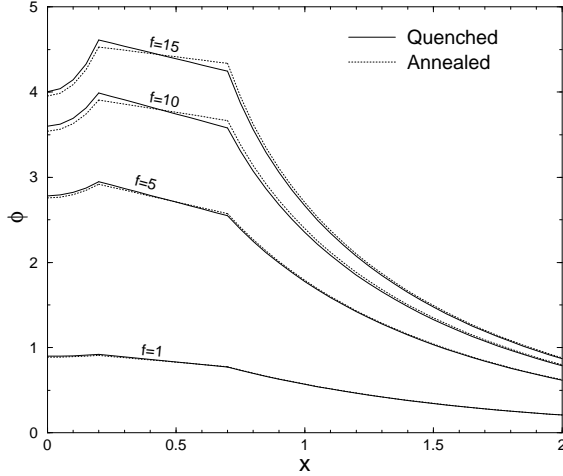


Figure 5: Comparison of the local electrostatic potential $\phi(x)$ for the quenched and annealed cases. The geometric parameters are same as in figure 4. Moderate difference is only observed for $f \gg 1$ in accordance with figure 3.

dotted line represents the corresponding linear DH mean potential. Even though for $f \ll 1$ both theories coincide, DH theory fails to quantitatively predict the local value of the mean field for $f \gtrsim 1$. For example, for $D \rightarrow 0$, (20) reduces to $\phi_0 = (f_i + f_o)e^{-H/2}$, thus, the total charge density $\sigma_i + \sigma_o$ is concentrated in a plane of infinitesimal width and the potential at the plane of symmetry decreases exponentially with respect to the plates separation. In the limit $D \rightarrow \infty$ we have $\phi_0 = f_i / \sinh(H/2)$, this expression diverges for $H \rightarrow 0$ whereas eq. (17) predicts a finite value for this quantity. In figure 5, we compare the electrostatic field in the quenched case with that in the annealed case. Notice that as charge moves from the inner to the outer surface, the potential at the first decreases while it increases at the later. In other words relaxation of charge reduces the potential difference between the inner and outer surfaces. This effect is stronger for larger f in accordance with figure 3.

5.3 Force between the colloids

The pressure is the force between the plates per unit area, and is defined in terms of the grand potential through the relation $\beta p / (2\rho_s) = -\partial\omega / \partial H$. Alternatively, taking into account the fact that the electrostatic pressure of the system must balance the hydrostatic pressure, it can be written in terms of the mean field ψ as [1]

$$p = k_B T (n(x) - 2\rho_s) - \frac{\varepsilon}{8\pi} \left(\frac{d\psi}{dx} \right)^2 + \frac{\varepsilon}{8\pi} \left(\frac{d\psi}{dx} \right)^2_{H \rightarrow \infty} \quad (24)$$

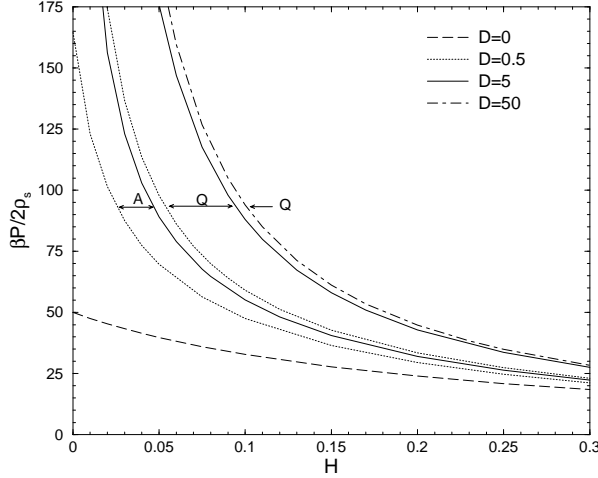


Figure 6: Dimensionless force per unit area between the colloids for $f = 10$. This quantity is always positive, indicating repulsion between the colloids, and tends to zero for as the separation between the colloids increases. The plots for the quenched and annealed cases are labelled with Q and A respectively.

where $n(x) = \rho_+(x) + \rho_-(x)$ is the total density of microions at x . It is easy to show that within PB theory, this quantity gives the same value for any position x . In particular evaluating at $x = 0$ we get

$$\beta p = 2\rho_s(\cosh \phi_0 - 1), \quad (25)$$

which implies that the force between the colloids is completely determined by the value of the mean electrostatic potential at the plane of symmetry. This feature allow us to find this quantity directly from the numerical solution of equation (17). In figure 6 we plot the dimensionless pressure as a function of the colloidal separation, for different values of the thickness D for the quenched and annealed cases. Although the last two give obviously the same curve for $D = 0$, a substantial difference is observed for small, nonzero, colloidal thicknesses. On the other hand, for $D = 10$ and larger, the inter-colloidal force turns out to be almost independent of the thickness for the same reasons discussed before in the context of charge relaxation. All the curves tend asymptotically to zero in the limit of infinite colloidal separation. In the DH limit $\beta p = 2\rho_s(\cosh \phi_0 - 1) \simeq \rho_s \phi_0^2$. Using (20) we obtain $\beta p = \rho_s f_i^2 / \sinh^2(\frac{H}{2})$ for $D \rightarrow \infty$. Again, in the limit $H \rightarrow 0$, the linear theory predicts divergent behavior for the pressure, while the full nonlinear theory gives a finite value for this quantity.

5.4 Average charge density between the colloids

Using Poisson's equation $\phi''(x) = -\rho(x)/(2\rho_s)$, we compute the ratio $\langle Q \rangle$ of the average ion charge density between the two colloids, compared to the charge

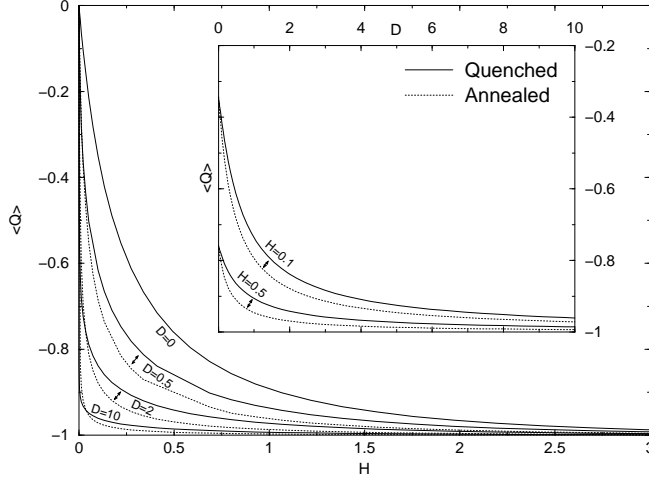


Figure 7: Average charge density in the region between the colloids for $f = 10$. When $D \rightarrow \infty$ charge of sign opposite to that on the colloidal surface is present in the middle region to neutralize the charge on the colloids. When D is finite, part of that charge is squeezed out of the middle region as the colloids are driven to a closer relative position. The insert shows the squeezing of charge when we decrease the thickness for fixed separation H .

density on the inner faces of the colloids:

$$\langle Q \rangle = \frac{e}{\kappa\sigma_i} \int_0^{H/2} \rho(x) dx = \frac{1}{f_i} \left(\phi'(0) - \phi'\left(\frac{H}{2}\right) \right) = -\frac{\phi'\left(\frac{H}{2}\right)}{f_i}. \quad (26)$$

This quantity is shown as a function of the inter-colloidal distance for different values of D in figure 7. When the distance between the finite-width colloids is shortened, charge can be squeezed out of the region between the colloids. This is not possible for semi-infinite colloids, since in that case there is no place for the charge to be squeezed out, such that $\langle Q \rangle = -1$ for all H as shown in figure 7. The inset shows the squeezing of charge when we decrease the thickness for fixed separation H . For $D = 0$ the quenched and annealed cases coincide. One expects that Q is closer to -1 in the annealed case than in the quenched case, since the surface charge can follow the squeezed-out ionic charge by migration to the outer surface. This is indeed shown by our numerical results as shown in figure 7. However, for very small separations, $H \approx 10^{-2}$ this effect is reversed, as can be seen in figure 8, where $\langle Q \rangle$ is closer to -1 in the quenched case. Note that this effect occurs for rather small values of the separation distance. In a model that accounts for the finite-size of the ions this effect is presumably absent.

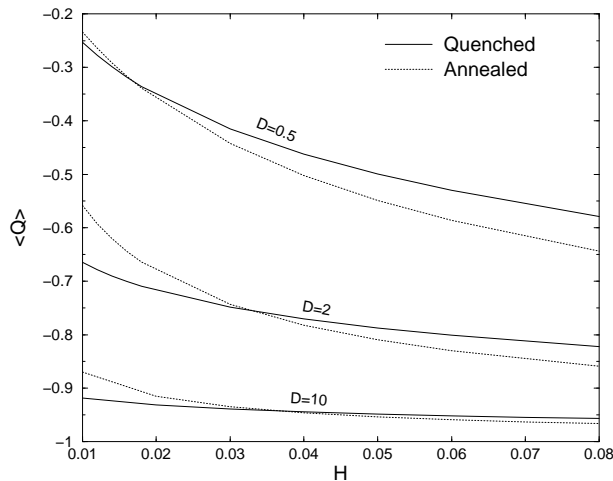


Figure 8: Average charge density (see text) in the region between the colloids for $f = 10$.

6 Conclusion

The system consisting of two interacting double-layers, used as a model of colloidal interactions when the curvature of the macromolecules is negligible has been extended to consider finite-width colloids, by the inclusion of two additional interacting double layers. The force that drives the colloidal particles apart is modified by their finite-size. The nonlinear PB equation was solved considering this finite-size to find quantitatively the dependence of the mean field with respect to the geometrical parameters. We considered two relevant cases: the quenched case where the surface charge density on each surface of the colloids is the same and the annealed case, where the total charge of each colloid is fixed, but not the charge on each surface. In the latter case a charge “relaxation” effect is possible where the charges in each surface rearrange themselves in order to minimize the grand potential of the system. We found that this relaxation effect modifies also the mean electrostatic potential, and as a consequence the force between the colloids. We consider these results as a stepping stone towards the study of more complicated charge-relaxation and charge-regularization mechanisms, and to more complicated geometries, such as spheres treated within the Derjaguin approximation.

7 Acknowledgments

This work is part of the research program of the Stichting voor Fundamenteel Onderzoek der Materie (FOM), which is financially supported by the Nederlandse Organisatie voor Wetenschappelijk Onderzoek (NWO). G. T. acknowl-

edges partial financial support from COLCIENCIAS project 1204-05-13625.

References

- [1] E. J. W. Verwey and J. Th. G. Overbeek, *Theory of the stability of lyophobic colloids* (Elsevier, Amsterdam, 1948).
- [2] B. W. Ninham and V. A. Parsegian, *J. Theor. Biol.* **31**, 405 (1971).
- [3] S. H. Behrens and M. Borkovec, *Phys. Rev. E* **60**, 7040 (1999).
- [4] S. Alexander, P. M. Chaikin, P. Grant, G. Morales, P. Pincus, and D. Hone, *J. Chem. Phys.*, **80**, 5776 (1984).
- [5] E. Trizac, L. Bocquet and M. Aubouy, *Phys. Rev. Lett.* **89**, 248301 (2002).
- [6] L. Bocquet, E. Trizac, M. Aubouy, *J. Chem. Phys.* **117**, 8138 (2002).
- [7] E. Trizac and Y. Levin, *Phys. Rev. E*, **69**, 031403 (2004).
- [8] D. McCormack, S.L. Carnie, and D. Y. C. Chan, *J. Colloid Interface Sci.* **169**, 177 (1995).
- [9] M. N. Tamashiro and H. Schiessel, *Phys. Rev. E* **68**, 066106 (2003).
- [10] I. S. Gradshteyn, I. M. Ryzhik, *Table of Integrals, Series, and Products* (Academic Press 1994).
- [11] All the numerical resolutions (root finding and minimization) involving the Jacobian elliptic functions were performed using MATHEMATICA version 5.
- [12] E. T. Whittaker and G. N. Watson, *A course of modern analysis*, (Cambridge, 1927)